Ultra Low Power Cryo-Refrigerator for Space Applications

M.V. Zagarola, R.W. Hill, J.R. Gagne, R.W. Kaszeta

Creare, Hanover, NH, USA 03755

ABSTRACT

Future NASA astronomical observatories will require long-life, mechanical cryocoolers to cool bolometers, detectors, sensors, shields, and telescopes. Some missions will be flown to either the outer planets, or the L2 Lagrange point. Here, the scientific payload can be effectively shielded from the sun and earth which reduces thermal noise and parasitics, but power is more difficult to generate due to the reduced solar flux. Consequently, payload power and mass are even more critical parameters for these observatories than for earth-orbiting satellites. Creare has developed a reverse Brayton cryocooler design that meets aggressive mass and input power objectives. The cryocooler has been optimized to provide 300 mW of cooling at 35 K and requires 8.9 W of compressor input power at 150 K. The total system mass is 6.2 kg including electronics and cryo-radiator. The cryocooler is designed to operate at cold end temperatures of 30 to 70 K, loads of up to 3 W, and heat rejection temperatures of up to 210 K by changing only the charge pressure and turbomachine operating speeds. On a recent project, a technology demonstration cryocooler was built and tested over a range of cold end temperatures. In addition, a key cryocooler component, the recuperator/turboalternator assembly, was mechanically tested for tolerance to launch vibration. The design of the cryocooler and results of the testing are the subjects of this paper.

INTRODUCTION

Future NASA space science missions will require long-life cryocoolers for cooling bolometers, detectors, sensors, shields, and telescopes. Some of these missions are either to the outer planets or to the L2 Lagrange point, a metastable orbit located 1.5 million kilometers beyond earth's orbit. Here, the scientific payload can be effectively shielded from the sun and earth which reduces thermal noise and parasitics, but power is more difficult to generate due to the reduced solar flux. Consequently, payload power and mass are even more critical parameters for these observatories than for earth-orbiting satellites.

The development of current cryocooler technology for space has been driven almost exclusively by satellites in low earth and geosynchronous orbits where spacecraft heat rejection temperatures are typically 300 K to 320 K. The recent Planck observatory [1] operated and the future James Webb Space Telescope [2] will operate in an L2 orbit, but will utilize cryogenic systems that reject most of their waste heat at temperatures near 300 K. The process of pumping heat from an extremely low to high temperature is thermodynamically inefficient and results in excessive input power and payload mass. Conversely, rejecting heat at cryogenic temperatures

Cryocoolers 18, edited by S.D. Miller and R.G. Ross, Jr.

requires cryogenic radiators which increase in size inversely with rejection temperature to the fourth power. These competing effects should be considered during payload trade studies, but the lack of an efficient cryocooler that can operate with a cryogenic heat rejection temperature has prevented meaningful mission studies in this area. Creare's circulators and turboalternators have already been demonstrated on prior space programs to operate at cryogenic temperatures [3]. The application of our turbomachine technology to a cryo-compressor is an enabling technology and a natural extension of this prior work.

In this paper, we describe the development and demonstration of an innovative turbo-Brayton cryocooler that takes advantage of the unique thermal environment associated with deep-space missions. In particular, the cryocooler utilizes a cryogenic heat rejection temperature to dramatically reduce payload input power, size, and mass. Our cryocooler is predicted to reduce cryocooler input power by an order of magnitude as compared to the current state-of-the-art cryocooler.

ULTRA LOW POWER (ULP) CRYOCOOLER

The cryocooler concept is shown conceptually in Figure 1: a single-stage turbo-Brayton cryocooler operates between a cryogenic heat rejection temperature and the primary load temperature. The key cryocooler components are a cryogenic compressor, a recuperative heat exchanger (i.e., recuperator), and a turboalternator. The cryogenic compressor and turboalternator are gas bearing turbomachines that are extremely reliable and produce no perceptible vibration. The continuous flow nature of the cycle allows the cycle gas to be transported from the compressor outlet to a heat rejection radiator at the warm end of the cryocooler, and from the turboalternator outlet to the object to be cooled at the cold end of the cryocooler. The unit shown in Figure 1 has been optimized to provide 300 mW of cooling at 35 K and rejects 8.9 W of heat at 150 K. The electronics have been designed for operation in high-radiation environments. The total system mass is 6.2 kg including electronics and cryo-radiator. The cryocooler is designed to operate at cold end temperatures of 30 to 70 K, loads of up to 3 W, and heat rejection temperatures of up to 210 K by changing only the charge pressure and turbomachine operating speeds. The enabling technology for this concept is a cryogenic compressor that has heritage to the NICMOS circulator [3].

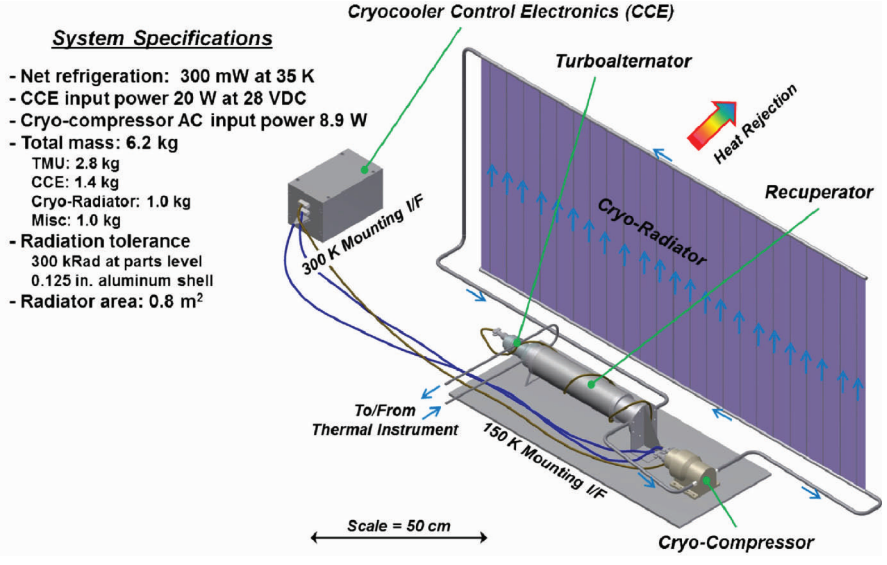

Figure 1. An ultra low power cryo-refrigerator for space.

Table 1 provides a comparison of the predicted performance and mass of the flight ULP cryocooler with the actual values for the current state-of-the-art cryocoolers. The current state-of-the-art includes three low capacity single-stage cryocoolers with operational data in the 35 K to 40 K range and a heat rejection temperature of 300 K. The comparison in Table 1 shows that the proposed cryocooler is a factor of two more efficient than the current state-of-the-art cryocoolers, and requires significantly less input power due to the higher efficiency and reduced heat rejection temperature. In addition, the proposed cryocooler is 43% lighter than the lightest existing space cryocooler. Even after accounting for the mass of the cryo-radiator and integration hardware (2.0 kg), our proposed concept is 16% lighter. Additional reductions in payload mass will be realized because of smaller heat rejection radiators at 300 K and smaller power sources whether radioisotope or solar. The performance map for the cryocooler is shown in Figure 2.

Table 1. Comparison of Low Capacity Single-Stage 35 K Cryocoolers.

Vendor	Technology	Cryocooler Mass	Comp. Input Power/ Heat Rej. Temp.	Refrigeration	% Carnot
Northrop Grumman [4]	Pulse Tube	7.4 kg	88 W at 300 K	750 mW at 40 K	5.5%
BATC [4]	Stirling	14.6 kg	74 W at 300 K	590 mW at 35 K	6.8%
Raytheon [4]	Stirling	20.1 kg	133 W at 300 K	1300 mW at 35 K	7.4%
Creare Flight ULP Prediction	Brayton	4.2 kg	8.9 W at 150 K	300 mW at 35 K	11%

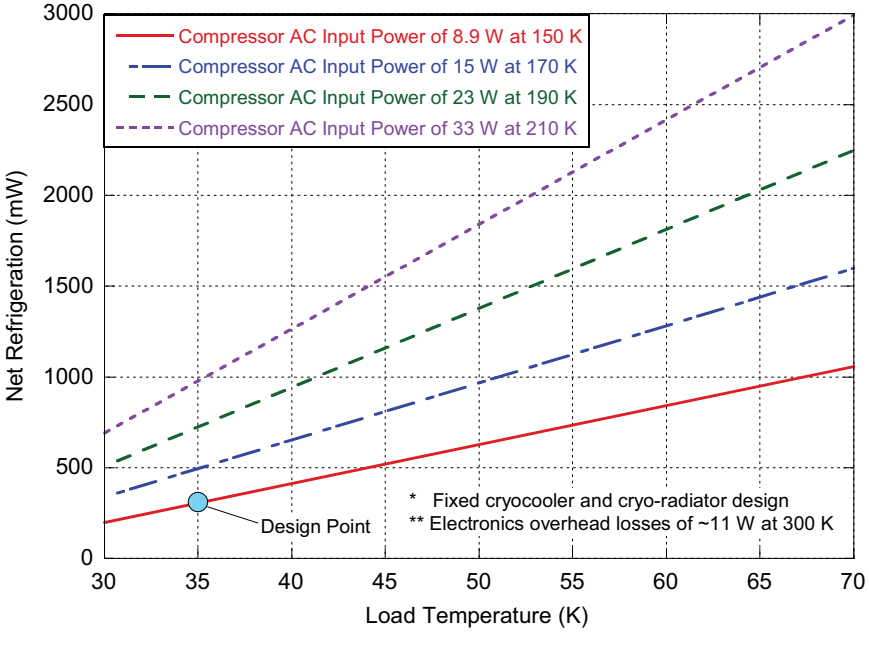

Figure 2. Cryocooler performance map.

Creare recently completed a project to demonstrate the ULP cryocooler technology. We built and tested a Technology Demonstration Unit (TDU) that consists of prototypical cryocooler components, rack-mounted electronics, and a prototypical cryo-radiator. A comparison of the flight system and TDU are given in Table 2. To reduce program costs, the TDU uses existing components for the cryo-compressor and turboalternator. The cryo-compressor is a spare unit from the NICMOS program [3] with adjustments to the bearing clearances for higher operating speeds consistent with a compressor. The turboalternator is our ultra-low capacity (ULC) model [5] with modifications to the external features to reduce rotor bypass leakage, a performance penalty. The recuperator is a new unit based on our silicon slotted plate technology [6]. The TDU and flight recuperators are expected to be identical. The recuperator and turboalternator are an integrated assembly to reduce thermal parasitics to the cold end. The radiator is a new design where the cycle gas flows directly through tubes that are brazed to a stainless steel panel. The tubes and panel have been designed for micro-meteorite tolerance consistent with long-duration deep space missions. The TDU and flight radiators are expected to be identical except for the configuration of the panels. The panels were configured in a pentagon for the TDU to fit within an existing thermal vacuum chamber. The electronics for the TDU are rack-mounted with manual controls. This approach was taken for the TDU electronics since the radiation tolerance requirements vary significantly for the different missions and building a set of electronics for the worst case was not cost effective. The net result of these modifications is that the predicted performance of the TDU is nominally 7% of the Carnot cycle as compared to 11% for the flight unit.

CRYOCOOLER TESTING

The cryocooler was performance tested at design and off-design operating conditions to map performance. The cryocooler and all components met or exceeded performance expectations. In addition, the recuperator assembly was vibration tested up to 12.4 Grms without failure. Details of the cryocooler performance test and the vibration test on the recuperator assembly are given in the following subsections.

Performance Test Configuration

The cryocooler was performance tested at Creare in April 2014. The test set-up within the thermal vacuum chamber is shown in Figure 3. A cycle schematic with the measurement

Table 2. Flight System to Phase II Technology Demonstration Unit Component Differences.

Component	Flight System	Technology Demo Unit
Turboalternator	ULC Turboalternator with reduction of rotor bypass leakage, upgraded aerodynamics and stator material	ULC Turboalternator with reduction of rotor bypass leakage w/o upgrades to aerodynamics and stator material
Cryo-compressor	Low capacity design with same internals as ULC turboalternator but with optimized compressor aerodynamics	NICMOS circulator FM Unit #2 with bearings adjusted for higher speeds
Recuperator	New design - 260-plate silicon recuperator integrated with turboalternator housing	Same as flight
Cryo-radiator	New design - Flat panel radiator with stainless tubes, fins, and header with high emissivity coating	Same as flight but segmented to fit inside existing thermal vacuum chamber
Control Electronics	Custom boards optimized for cryo-refrigerator with >300 kRad components	Creare laboratory electronics

locations is given in Figure 4. The cryocooler system comprises a cryo-compressor, recuperator, turboalternator, precooler heat exchanger, cold load interface heat exchanger, and radiator. The cycle gas was neon. The component assemblies were connected by stainless steel and/or titanium tubing. The refrigeration load temperature at the load interface heat exchanger was maintained using an electric trim heater. The cryocooler heat rejection temperature was allowed to float based on the thermodynamic operating conditions of the cryocooler, the shroud temperature and heat load applied to the mounting plate heater (Q3).

The cryocooler and cryo-radiator were installed within the cold thermal shroud of the test chamber. The thermal shroud was actively cooled between 100 K and 140 K using a Gifford-McMahon cryocooler and trim heaters, and was supported using low-conductivity struts from the baseplate of the bell jar. The bell jar was evacuated using a turbo-molecular pump. The exterior of the cold shroud was wrapped in modular multi-layer insulation (MLI) to minimize radiation to the warm bell jar. The outer surface of the radiator panels faced outward toward the cold shroud which was coated with the same high emissivity paint as the radiator. Within the cold-shroud, the cryocooler components were wrapped in MLI to minimize radiation to the cold shroud. The inward-facing side of the radiators was also covered with MLI so that the only radiation path was outward to the cold shroud.

The cryo-compressor, recuperator, turboalternator and precooler heat exchanger were mounted to an aluminum plate, as shown in Figure 5, which was supported in the cold shroud using low conductivity struts. A copper strap was wrapped around the cryo-compressor housing and bolted to the aluminum plate to transfer dissipation from the compressor motor and bearings to the plate, and a precooler heat exchanger was mounted to the plate to transfer the dissipation of the compressor into the cycle gas. The recuperator warm end bracket and cold end flexure were also bolted to the plate. The turboalternator was integral to the cold end of the recuperator.

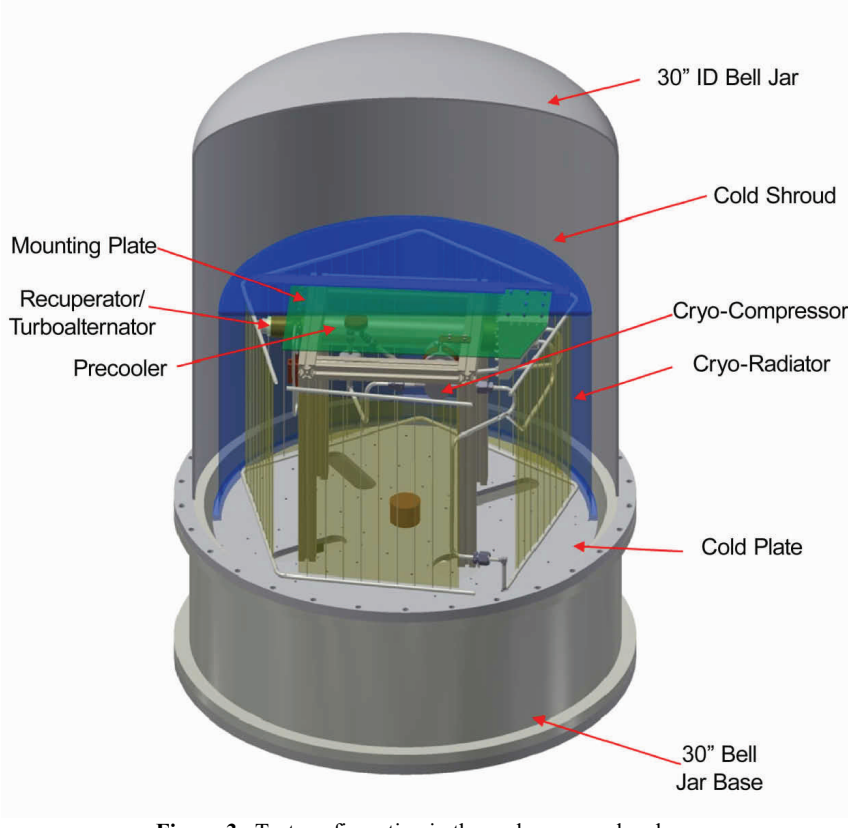

Figure 3. Test configuration in thermal vacuum chamber.

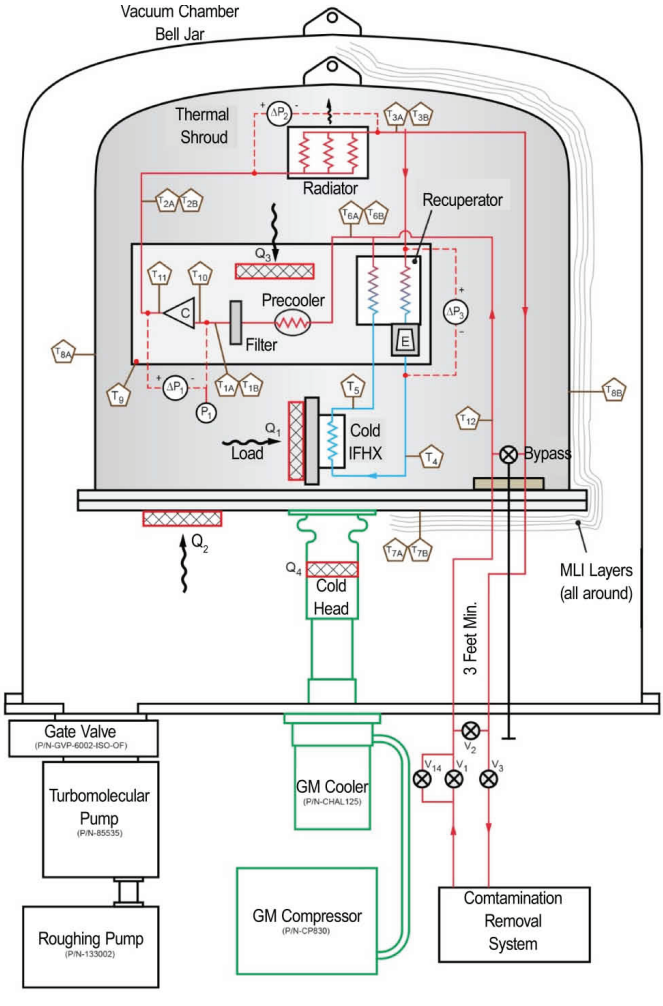

Figure 4. Test facility and system schematic.

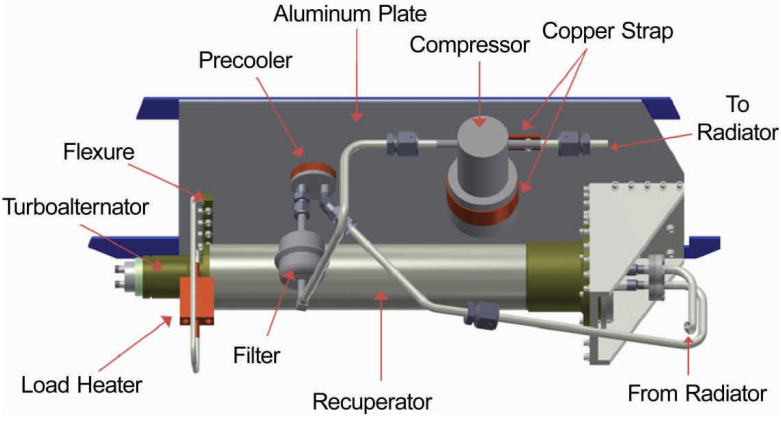

Figure 5. Configuration of primary mechanical cryocooler components.

Performance Testing

In Figure 6, the net refrigeration is plotted as a function of load temperature. The net refrigeration increases linearly with load temperature. The minimum and maximum refrigeration was 277 mW at 35.0 K and 550 mW at 40.5 K, respectively. For these four test points, the compressor AC input power was fixed at 17.7 W, the shroud temperature was fixed at 118 K and the radiator return was fixed at 150 K. The target refrigeration of 300 mW at 35 K is also shown in Figure 6. The cryocooler refrigeration was 23 mW below the target refrigeration. The target refrigeration could be met with a 10% reduction in parasitics through improved insulation or a 3% increase in input power.

The figure of merit for a cryocooler is the Carnot efficiency (η_{Carnot}), which is the coefficient of performance (COP) for the cryocooler (cooling capacity divided by input power) divided by the COP of an ideal Carnot cycle operating at the same temperatures. That is:

$$\eta_{Carnot} = \frac{Q_{load}}{W_{AC,c} - W_{AC,t}} \left(\frac{T_{reject}}{T_{load}} - 1 \right) \tag{1}$$

where T_{reject} is the heat rejection temperature taken to be the radiator outlet temperature, and T_{load} is the cooling load temperature taken to be the load outlet temperature. The COP of the cryocooler relative to the Carnot cycle is shown in Figure 7. The measured Carnot efficiency increases with refrigeration from 5.5% for 277 mW at 35.0 K to 9.1% at the maximum load case of 550 mW at 40.5 K. Also shown in Figure 7 is the Carnot efficiency if we are able to reduce thermal parasitics by 70% through improved insulation or operation at a lower heat sink (shroud) temperature to reduce parasitics. Testing at different shroud and mount plate temperatures indicated that the radiative parasitics from the shroud and conductive parasitics from the mount plate were significant and typically a factor of 5 greater than predictions. A post-test inspection revealed several areas where insulation could be improved if testing was performed in a larger chamber.

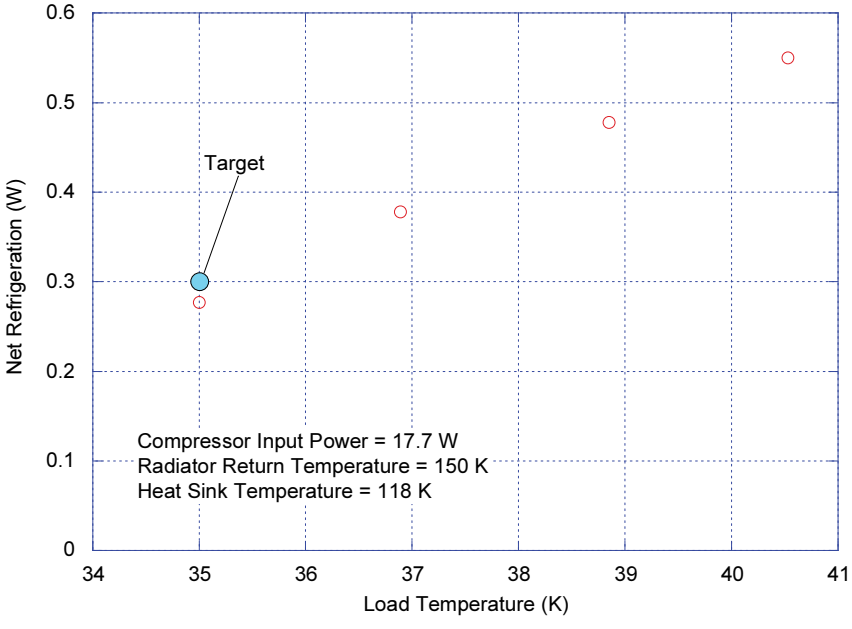

Figure 6. Net refrigeration as a function of load temperature for fixed input power, heat rejection temperature and heat sink temperature.

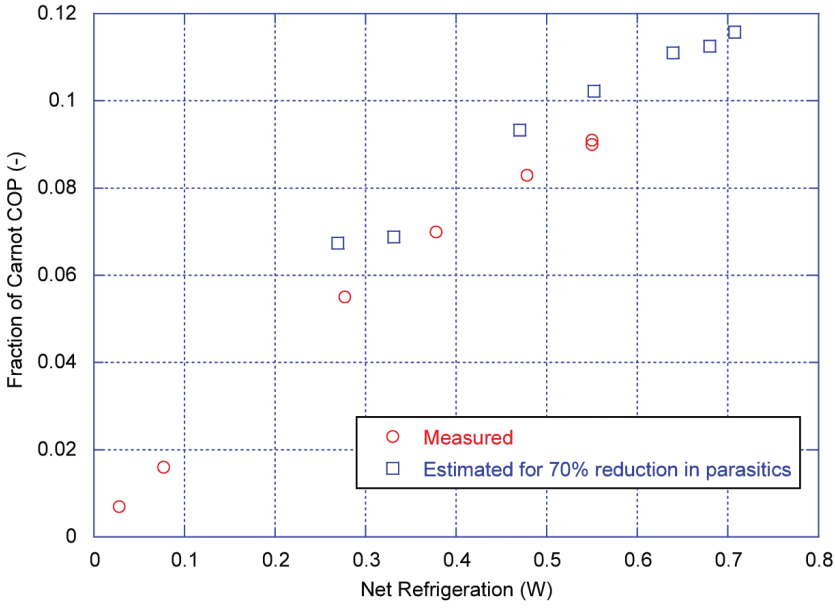

Figure 7. Cryocooler performance relative to the Carnot cycle.

Vibration Testing

Another goal of the project was to increase the technology readiness level (TRL) of the mechanical cryocooler to 5/6 by testing in an operational environment. This maturity level is achieved through performance testing in a thermal vacuum chamber and launch vibration testing using a shaker table. For the ULP cryocooler, the cryo-compressor was previously flight qualified during the NICMOS program, and the turboalternator is a 2/3-scale version of the unit qualified on the NICMOS program. Therefore, these components were not tested on the current program. The recuperator and cryo-radiator are new technologies and are structurally sensitive. The radiator is designed for mounting on the outer surface of a spacecraft and not intended to endure vibration as a stand-alone component. In addition, the cryo-radiator for the TDU was configured in 5 panels to fit within the thermal shroud of the test chamber, precluding vibration testing on this component. Therefore, our vibration testing focused on the recuperator assembly.

Testing was performed in the flight configuration shown in Figure 8. The recuperator assembly consisted of the recuperator, cold-end flexure, warm-end rigid mount, and a turboalternator simulator. The warm-end rigid mount was designed for high stiffness to provide a well-defined boundary condition, and is not intended for space flight. For a flight system, the warm-end bracket is expected to be a lightweight beryllium structure, or alternatively, the recuperator assembly would be mounted directly to the payload. A turboalternator simulator was utilized instead of the turboalternator to allow isolation of the high-pressure and low-pressure flow paths from one another and to permit cross-stream leak tests. The simulator had the same mass (280 g) and center of gravity as the turboalternator assembly which it replaced.

Mechanical failure of the recuperator was assessed between and after vibration tests by a change in the primary resonant frequencies, inability to hold pressure, or an increase in the cross-stream leakage above the baseline value ($< 1\times10^{-4}$ g/s of helium at a 10 psid pressure difference). A change in resonant frequency would indicate failure of the cold end flexure, recuperator shell or recuperator core. An inability to hold pressure would indicate a failure of the pressure boundary which includes the recuperator shell. An increase in the cross stream leakage above the baseline value would indicate a failure of the recuperator core.

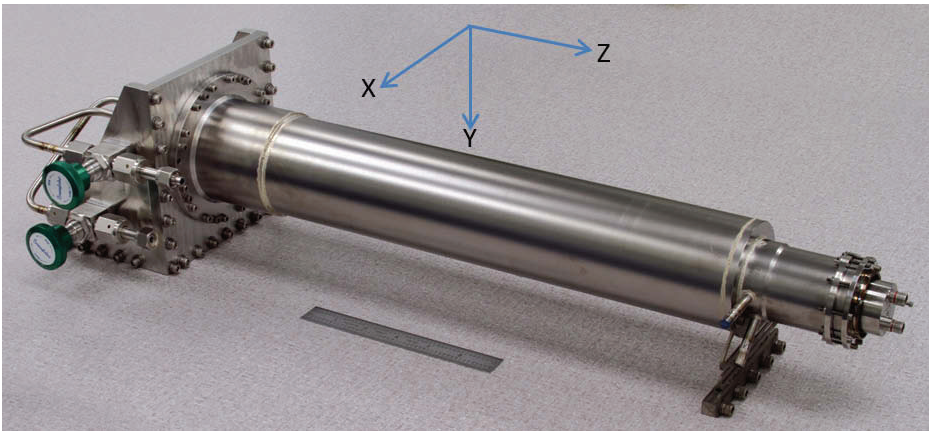

Figure 8. Photograph of recuperator/turboalternator assembly mounted with cold end flexure and warm end bracket.

The vibration test consisted of characterization tests to determine the structural response of the recuperator and random vibration tests to verify that the recuperator meets typical random vibration requirements for space flight. The characterization tests were performed in all three axes. The random vibration tests were performed in the transverse (X) and axial (Z) axes at -6 dB, -3 dB and -1 dB relative to the NASA GEVS qualification spectrum (14.1 Grms). The recuperator was not tested at 0 dB relative to the spectrum due to limitations of the shaker table. In addition, a notch to the spectrum was applied in the transverse direction at the lowest resonant frequency of the recuperator assembly (nominally 100 Hz) due to low measured damping and concerns with failure of the cold-end flexure. The thickness of the flexure could be increased to reduce stresses at the expense of increased heat leak (currently 23 mW), but this was not pursued on the current program. Due to spectrum notching and shaker table limits, the random vibration testing was performed at a maximum level of 12.5 G_{rms}. The input spectra are given in Figure 8. The recuperator successfully survived random vibration testing up to 12.4 G_{rms} in the transverse axis and 12.5 G_{rms} in the axial axis with no evidence of mechanical damage.

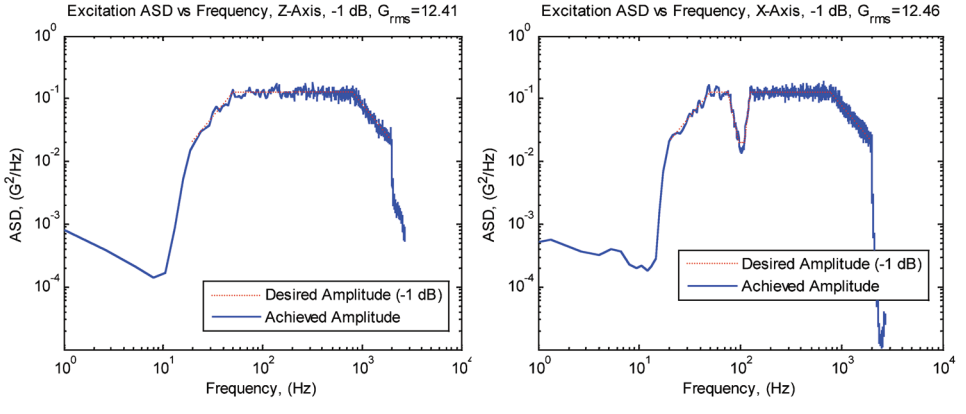

Figure 9. Measured and desired input spectra in axial (z, left) and transverse (x, right) axes for random vibration testing of the recuperator assembly.

CONCLUSIONS

Creare recently built and tested a technology demonstration unit for an ultra-low power cryocooler. The unit comprised an existing cryo-compressor and turboalternator, and new components for the recuperator and cryo-radiator. Thermal vacuum test results were excellent. The cryocooler produced 280 mW to 550 mW of net refrigeration at load temperatures from 35.0 K to 40.5 K. The AC electrical input power was less than 18 W at a heat rejection temperature of 150 K. The peak efficiency was 8.4% relative to the Carnot efficiency. All components met or exceeded performance expectations. Improvements to the multi-layer insulation were also identified that could significantly increase net refrigeration. In addition, the recuperator assembly was vibration tested up to 12.4 Grms without failure.

The work completed on this program increased the TRL of the technology from 4 to 5/6. The measured efficiency of this cryocooler compares favorably to existing 35 to 40 K, as shown in Table 1, even at lower refrigeration values. This level of performance was achieved on a non-optimized version of the cryocooler that utilized mostly existing components. Further optimization for the flight unit is expected to improve performance up to the flight predictions. The next step for the technology would be to build and test an optimized engineering model cryocooler for a particular mission or mission class. The overall mass of the flight cryocooler, cryo-radiator and electronics is predicted to be 6.2 kg, the area of the cryo-radiator is 0.8 m^2 and the input power to the compressor is predicted to be less than 9 W. The input power is an order of magnitude less than current state-of-the-art cryocoolers that utilize a 300 K heat sink.

ACKNOWLEDGEMENTS

The support and guidance from NASA-GSFC are gratefully acknowledged (Contract NNX12CA39C).

REFERENCES

1. Bernard, C., Martin, L., and Nicola, R., “Herschel-Planck, and the Next Steps in Space Cryogenics,” *19th International Cryogenic Engineering Conference*, Paper 1083, Grenoble, France, Narosa Publishing House, New Delhi, India, 2002, pp. 1–11.
2. Durand, D., Adachi, D., Harvey, D., Jaco, C., Michaelian, M., Nguyen, T., Petach, M., and Raab, J., “Mid InfraRed Instrument (MIRI) Cooler Subsystem Design,” *Cryocoolers 14*, ICC Press, Boulder, CO (2007), pp. 7–12.
3. Swift, W. L., Dolan, F. X. and Zagarola, M. V., “The NICMOS Cooling System—5 Years of Successful On-Orbit Operation,” *Adv. in Cryogenic Engineering*, Vol. 53, Amer. Institute of Physics, Melville, NY (2008), pp. 799–806.
4. Curran, D. G., Cha, J. S., and Yuan, S. W., “Space Cryocooler Vendor Survey Update: 2007,” TOR-2008(1033)-7691, The Aerospace Corporation, El Segundo, CA, January 2008.
5. Zagarola, M.V., McCormick, J.A., and Cragin, K.J., “Demonstration of an Ultra-Miniature Turboalternator for Space-Borne Turbo-Brayton Cryocooler,” *Cryocoolers 17*, ICC Press, Boulder, CO (2013), pp. 453 – 460.
6. Hill, R. W., Izenson, M. G., Chen, W. and Zagarola, M., “A Recuperative Heat Exchanger for Space-Borne Turbo-Brayton Cryocoolers,” *Cryocoolers 14*, ICC Press, Boulder, CO (2007), pp. 525–533.